

# Conversion Analysis of Acrylated Hyperbranched Polymers UV-Cured Below Their Ultimate Glass Transition Temperature

Lars Erik Schmidt,<sup>1</sup> Yves Leterrier,<sup>1</sup> Daniel Schmä, <sup>1</sup> Jan-Anders E. Månson,<sup>1</sup> David James,<sup>2</sup> Eva Gustavsson,<sup>2</sup> Lennart S. Svensson<sup>2</sup>

<sup>1</sup>Laboratoire de Technologie des Composites et Polymères, Ecole Polytechnique Fédérale de Lausanne, CH-1015 Lausanne, Switzerland

<sup>2</sup>Perstorp Specialty Chemicals AB, SE-28480 Perstorp, Sweden

Received 25 April 2006; accepted 10 November 2006

DOI 10.1002/app.25826

Published online in Wiley InterScience (www.interscience.wiley.com).

**ABSTRACT:** The photo-curing behavior of reactive blends of dipentaerythritol penta/hexaacrylate (DPHA) with an acrylated hyperbranched polyester and an acrylated hyperbranched polyether was investigated by means of photo differential scanning calorimetry. The chemical conversion data was analyzed using an autocatalytic model with close attention paid to the influence of composition, UV intensity, and vitrification. The autocatalytic model was found to be relevant to describe autoacceleration and diffusion controlled reaction stages, as long as the polymers were not vitrified. It was shown that the reaction order and the autocatalytic exponent were independent of UV inten-

sity, whereas the rate constant showed strong intensity dependence, and the maximal conversion showed weak intensity dependence. A criterion for vitrification onset was proposed as the occurrence of a third stage in the conversion process. The ultimate conversion was found to be 0.16 higher than the conversion at vitrification for all investigated multifunctional acrylates independent of composition and UV intensity. © 2007 Wiley Periodicals, Inc. *J Appl Polym Sci* 104: 2366–2376, 2007

**Key words:** acrylate; vitrification; photopolymerization; hyperbranched; glass transition

## INTRODUCTION

UV curing is mainly used in adhesives, coatings, and printing applications.<sup>1</sup> The advantages of UV curing are the absence of hazardous solvents and the short cycle times. Compared to their low functional counterparts, highly functional acrylates have the advantage that they cure at a lower light dose, which requires lower photoinitiator concentrations, weaker light sources, and results in faster line speeds.<sup>2</sup> They also have high ultimate glass transition temperatures, and form stronger and more impermeable coatings. However, their drawback is the large extent of polymerization shrinkage,<sup>3</sup> leading to defects such as cracking, bending, and delamination<sup>4,5</sup> and also causing significant surface roughness.<sup>6</sup> A promising means of reducing polymerization shrinkage is to use hyperbranched polymers (HBP) as pure products or in reactive blends.<sup>7–9</sup> This class of dendritic macromolecules has been widely studied as modifiers in a vast

range of thermosetting systems,<sup>10–12</sup> and to some extent in photosetting polymers.<sup>13–15</sup>

Understanding the network formation mechanisms of highly functional acrylates, including acrylated HBPs, helps to optimize material selection and to choose an appropriate curing process. A high ultimate conversion is desirable for good mechanical properties, barrier performance, and long-term stability. The kinetics of bulk photopolymerizations is a largely diffusion-controlled process. Parameters influencing the curing behavior include temperature, UV intensity, photoinitiator concentration, and the nature of the monomer. Cook<sup>16</sup> investigated the photopolymerization of bisphenol-A-dimethacrylate and found that the final degree of conversion was largely unaffected by variations in the initiation and polymerization rates, but was instead dependent on network mobility and hence on the curing temperature and resin structure. Specifically, Kou et al.<sup>17</sup> studied the influence of temperature, composition, and photoinitiator concentration on the photopolymerization of a reactive blend of an acrylated hyperbranched polymer with trimethylolpropane triacrylate (TMPTA). For a reactive blend of HBP with 20–60% of TMPTA, they found higher ultimate conversions compared to the pure products, which was attributed to differences in viscosity, unsaturation concentration, and network

Correspondence to: J.-A. E. Månson (jan-anders.manson@epfl.ch).

Contract grant sponsor: Swiss National Science Foundation; contract grant number: #2100.063675.00.

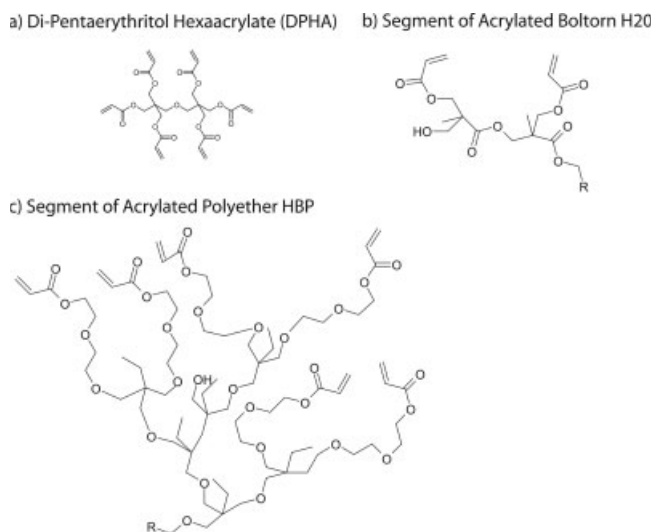


**Figure 1** Structures of the acrylate monomers. For the hyperbranched polymers (HBP), only one exemplary branch is shown. R denotes the core molecule from which four branches grow out. Reprinted from Ref. 21 with permission from Wiley-VCH.

morphology. In fact, little is known about the influence of intensity on the photopolymerization of acrylated HBPs. Similarly, the influence of network gelation and vitrification on the conversion process and ultimate conversion was not addressed.

During vitrification, the reaction rate slows down dramatically<sup>18</sup> and the material exhibits a complex time dependence behavior.<sup>19</sup> Especially in acrylates, vitrification is a gradual process, difficult to resolve.<sup>20</sup> Vitrification could be measured during UV curing for some acrylate monomers, depending on the ultimate  $T_g$  of the material, from rather complicated photorheology measurements<sup>21</sup>; therefore, it would be helpful to be able to identify vitrification from facile photo DSC measurements.

In this study, the UV curing behavior of highly functional acrylates and their reactive blends was investigated with close attention paid to the influence of intensity on the onset of vitrification.

## EXPERIMENTAL

Figure 1 depicts the structures of the different acrylate monomers studied, and Table I gives an overview over their physical and chemical properties. For the HBP, only one sample branch is shown. Dipentaerythritol penta/hexaacrylate (DPHA, UCB Chemicals) is an acrylate monomer with theoretically six functional groups but in reality and on average only five functional groups. Two HBP were also examined. The first one was based on a 16-hydroxyl functional second generation hyperbranched polyester (Boltorn<sup>®</sup> H20, Perstorp AB, Sweden) giving a 13-functional polyester acrylate called Acrylated Boltorn H20. The second one was based on a third generation hyperbranched polyether polyol (synthesized by Perstorp AB, Sweden) giving a 29-functional polyether acrylate called Acrylated Polyether HBP. Details of the synthesis and properties of these two HBPs can be found in the refs. 22,23.

The photoinitiator was 1-hydroxy-cyclohexyl-phenyl-ketone (Irgacure<sup>®</sup> 184, Ciba Specialty Chemicals) at a concentration equal to 1 wt %. It showed good solubility in the acrylate monomers. The small amount of photoinitiator should ensure a relatively homogeneous cure throughout the sample thickness.

The EFOS Novacure N2000 spotcure UV lamp was used to cure the samples. The UV-B portion (280–320 nm) of the lamp spectrum was about 22%, as determined via integration.<sup>21</sup> To measure the UV intensity, the Sola-Check sensor (Solatell, UK) was used. The UV lamp showed intensity variations of up to 20% between two illuminations.

The heat of the photopolymerization reaction was measured by means of photo-differential scanning calorimetry (photo-DSC, Perkin-Elmer DSC7, equipped with a UV-coupling cell). The cell comprised a lens, which focused the UV light onto the open aluminum sample pans. The sample holders were sealed with windows that let the UV light pass through to the sample and the reference. An IR filter was used to cut out the IR part of the lamp spectrum. The sample space was flushed with nitrogen. The

**TABLE I**  
Overview of the Physical and Chemical Properties of the Different Monomers Investigated

Property	Unit	DPHA	Ac. Boltorn H20	Ac. Polyether HBP
Core		Aliphatic	Polyester HBP	Polyether HBP
Theor. functionality		6	16	32
Actual functionality		5	13	29
Newtonian viscosity	(Pa s)	26	365	6
AEW	(g/mol)	104	316	294
DB (Fréchet)		–	0.8	0.35
$T_g$ monomer	(°C)	–36	–26	–55
$T_g$ polymer/at conversion	(°C)	68/73%	126/73%	28/83%
Acrylate concentration	(mmol/g)	8.0	4.8	3.4
Heat for 100% conversion	(J/g)	643.2	385.9	273.4

UV intensity was measured with the Solatell Sola-Check™.

To get a reference value of the heat of reaction for full conversion, the concentration of acrylate functions per weight, determined via titration, was multiplied by a reference value of 80.4 kJ/mol of acrylate functions<sup>24</sup> and the results are reported in Table I.

The viscosity of the monomers was measured with a Rheometric Scientific ARES rheometer using 25-mm parallel plates at the ambient temperature and an excitation frequency of 1 Hz. For DPHA, a viscosity of 26 Pa s was determined, for the Acrylate Boltorn H20, 365 Pa s, and for the Acrylated Polyether HBP, 6 Pa s.

The glass transition temperature ( $T_g$ ) of the monomers was measured by means of differential scanning calorimetry (TA Instruments Q100) at a heating rate of 10 K/min under  $N_2$  atmosphere. The glass transition temperature of the polymers cured under UV light (240 mW/cm<sup>2</sup>) was determined doing three-point bending tests on rectangular samples in a Rheometric Scientific RSA dynamic mechanical analyzer. Tests were performed at an excitation frequency of 1 Hz and a heating rate of 10 K/min, and the  $T_g$  was determined from the peak of  $\tan \delta$ .<sup>25</sup> The  $T_g$  of DPHA (73% conversion) was found to be equal to 68°C; the  $T_g$  of Acrylated Boltorn H20 (73% conversion) equaled 126°C; and the  $T_g$  of Acrylated Polyether HBP (83% conversion) equaled 28°C. For the Acrylated Boltorn H20 a very broad  $\tan \delta$  peak was found, spanning over more than 100°C, indicating an inhomogeneous network.<sup>25,26</sup>

The in-plane internal stress of acrylate coatings was determined from the curvature of coated aluminum beams, and calculated according to the model of Stoney.<sup>27</sup> The substrate was a 0.3 mm thick aluminum strip with a length of 180 mm and width of 8 mm, which was degreased and treated with a silane compound (2-propenoic acid, 2-methyl-, 3-(trimethoxysilyl)propyl, Silquest A-174<sup>®</sup>, GE Silicones) to promote adhesion of the acrylate coating. The acrylate was diluted in THF, applied on the aluminum strip, and the solvent was evaporated during 2 h at 80°C. The samples were produced in nitrogen atmosphere.

## RESULTS AND DISCUSSION

### Photocalorimetry analysis

Figure 2 shows the double bond conversion as a function of time and UV intensity for DPHA, Acrylated Boltorn H20 (polyester HBP), and Acrylated Polyether HBP. After a short induction time (less than 5 s), which was attributed to the formation of initiator-derived radicals and the inhibiting effect of dissolved oxygen, the reaction took off, and within

few seconds reached a conversion of about 30–50%, after which it considerably slowed down, eventually reaching a plateau value. The final conversion increased with intensity. This was explained by the fact that the shrinkage lagged back behind the conversion, the more so, the higher the intensity.<sup>28,29</sup> Therefore at higher intensities there was an excess mobility which enabled higher ultimate conversions to be reached. In the following, the maximum conversion is defined as the conversion for which the polymerization rate was smaller than 1% of the maximum polymerization rate.<sup>18</sup>

Comparing the three different monomers, it is evident that DPHA reached the lowest final conversion, followed by Acrylated Boltorn H20, and then Acrylated Polyether HBP, which achieved the highest final conversion. Two main factors contributed to these differences in final conversion. Firstly, higher ultimate  $T_g$  implies lower conversion at vitrification during isothermal cure below ultimate  $T_g$ , hence lower final conversion. The  $T_g$  of DPHA was found to be 40°C above the cure temperature (at 73% conversion), whereas in Acrylated Boltorn H20 it was 100°C above the cure temperature (also at 73% conversion). This also explains why vitrification of DPHA could be identified as a distinct event by means of photorheology,<sup>21</sup> whereas in Acrylated Boltorn H20 vitrification was a gradual process starting right after gelation. In the cured state, Acrylated Polyether HBP has a lower  $T_g$  (28°C) compared to that of Acrylated Boltorn H20 because the polyether core of Acrylated Polyether HBP is more flexible compared to the polyester core of Acrylated Boltorn H20.<sup>23</sup>

Secondly, compared to DPHA, Acrylated Boltorn H20 has an acrylate equivalent weight that is three times higher, which also contributed to its higher final conversion compared to that of DPHA. This result is supported by the work of Cook, who found that the rate of the propagation reaction decreased with decreasing length of the spacer group between methacrylate units.<sup>30</sup>

Figure 2 also shows the conversion rate as a function of double bond conversion for the three materials. In all cases, three main polymerization stages were identified. At the beginning of the reaction, a sharp increase in the rate of polymerization was evident, which corresponded to gelation or autoacceleration. In this first stage, no steady state could be identified in which the conversion rate stayed constant before autoacceleration set in. This does not agree with the findings of Kurdikar and Peppas,<sup>31</sup> who developed a model for diffusion-controlled photopolymerizations for diacrylate monomers. In the early stages of the reaction, the increasing viscosity significantly reduced the mobility of the long-chain radical species. Hence it was more unlikely for

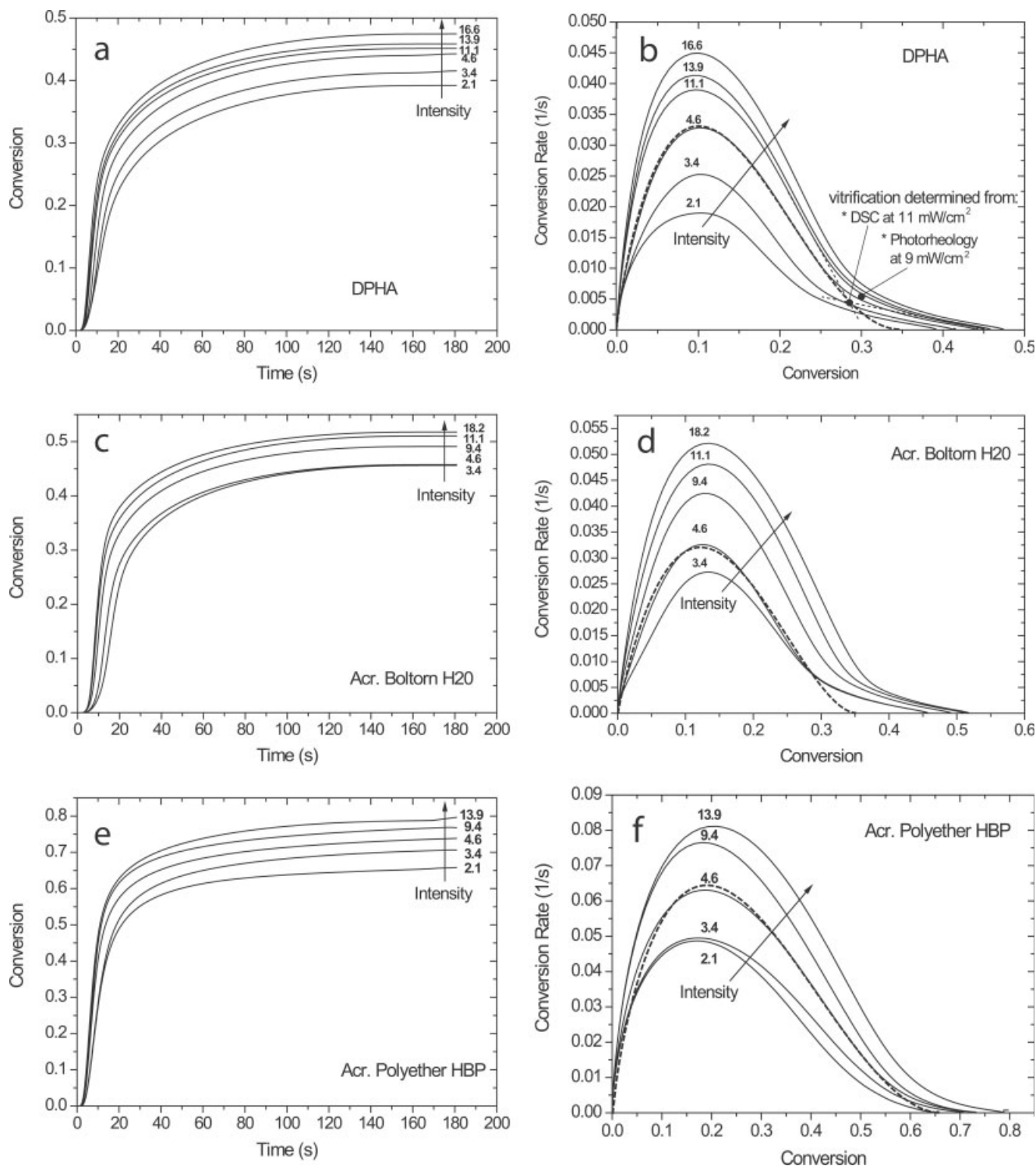


**Figure 2** (a, c, e) Double bond conversion as a function of time, and (b, d, f) conversion rate as a function of conversion for different UV intensities ( $\text{mW}/\text{cm}^2$ ) and materials. For DPHA the onset of vitrification is indicated. The autocatalytic model is also compared to the conversion rate data for an intensity of  $4.6 \text{ mW}/\text{cm}^2$ . The model was fitted to the data up to the vitrification onset and extrapolated beyond the vitrification onset back to zero conversion rate.

two radical species to approach each other and recombine. The rate constant for termination dropped dramatically,<sup>32</sup> and the rate of polymerization increased. The initiation and propagation steps were barely affected because the mobility of the small monomer

molecules was still high, even if viscosity of the reaction mixture was increasing.

The second stage started after going through a maximum rate of polymerization (reaction peak). In the case of DPHA and Acrylated Boltorn H20, conversion

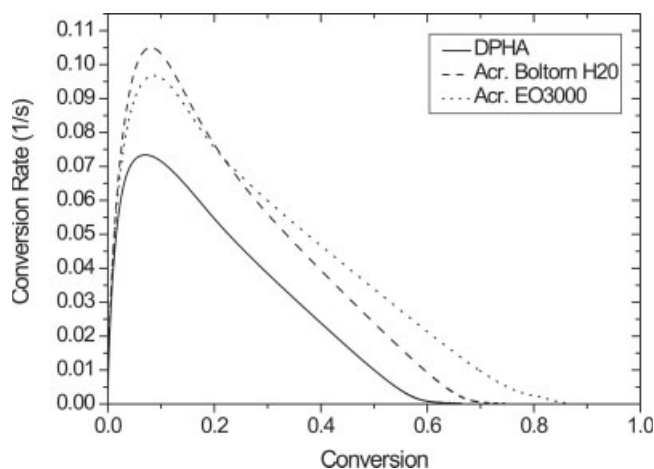


**Figure 3** Conversion rate as a function of conversion for the three different monomers cured at 79°C at an intensity of 20 mW/cm<sup>2</sup>.

at the reaction peak was equal to  $\sim 10\%$  and  $13\%$  respectively, and was found to be independent of intensity. In the case of the Acrylated Polyether HBP, the conversion at the reaction peak shifted from  $\sim 17\%$  ( $I = 2.1 \text{ mW/cm}^2$ ) to  $22\%$  ( $I = 13.9 \text{ mW/cm}^2$ ).

During the second stage, the reaction rate dropped quicker as would be expected from the consumption of monomers only<sup>33</sup> (autodeceleration), and the overall reaction became purely diffusion controlled. For Acrylated Boltorn H20 [Fig. 2(d)], the maximum reaction rates were about  $0.06 \text{ s}^{-1}$  higher compared to those of DPHA [Fig. 2(b)], and for Acrylated Polyether HBP [Fig. 2(f)] they were  $0.35 \text{ s}^{-1}$  higher than for Acrylated Boltorn H20. Again, the different molecular structures were responsible for that behavior. The kinetics of bulk photopolymerizations is a largely diffusion controlled process. The more flexible core of Acrylated Polyether HBP, compared to that of Acrylated Boltorn H20, facilitated diffusion.

In the third stage, which is evident for DPHA [Fig. 2(b)] and Acrylated Boltorn H20 [Fig. 2(d)] and less pronounced for Acrylated Polyether HBP [Fig. 2(f)], the reaction continued at a very low rate. This third stage may be attributed to vitrification, following a study by Yu et al.<sup>34</sup> A criterion for vitrification onset is proposed from the present results. It is defined as the crossover point,  $x_{vi}$ , of the tangent at the inflection point in the second stage, and the tangent to the third stage when the conversion rate  $dx/dt = 0.001 \text{ s}^{-1}$ . This criterion matches the photorheology analysis of these acrylate systems. In the case of DPHA, and under an intensity of  $9 \text{ mW/cm}^2$ , vitrification was measured after 17 s, corresponding to a conversion of  $29\%$ .<sup>21</sup> At  $11 \text{ mW/cm}^2$ , vitrification was determined at a conversion of  $28.5\%$  according to the present criterion.

Figure 3 shows the conversion behavior of the three monomers cured at 79°C, which was the maximum achievable temperature in the photo-DSC apparatus. It

is evident that the third stage in the rate profile is suppressed. This result confirms that the third stage is controlled by vitrification, in the case of curing below the ultimate glass transition temperature of the acrylate.

Figure 4 depicts the internal stress, calculated by Stoney's formula,<sup>27</sup> as a function of conversion. It was already stated by Payne<sup>35</sup> that significant stress develops only after half the final conversion is reached, and that after vitrification the conversion will only increase to a small extent, whereas the internal stress will increase greatly.<sup>36</sup> For very fast reacting systems, where internal stress is already measurable at early stages, Wen et al.<sup>37</sup> defined vitrification when the stress exceeded the linear extrapolation of the stress of the early reaction by  $0.1 \text{ MPa}$ . Following this approach, and as depicted in Figure 4, the conversion at vitrification  $x_{vi}$  was found to be equal to  $31\%$  for DPHA,  $34\%$  for Acrylated Boltorn H20, and  $52\%$  for Acrylated Polyether HBP. These values are very close to the values derived from the above photo-DSC data using the criterion proposed in the present study (cf. also Fig. 8).

The conversion profiles for reactive blends of DPHA with the two different HBPs are reproduced in Figures 5 and 6. Similar behavior, compared to that of pure products, is evident. Vitrification onset was systematically at higher conversion rates for the DPHA/HBP blends, compared to pure DPHA.

The influence of intensity and composition on the kinetics of photopolymerization will be discussed in detail in the following section, with close attention paid to the onset of vitrification.

### Conversion modeling

Conversion data obtained with Fourier transform IR spectroscopy (FTIR) or photo DSC can be analyzed

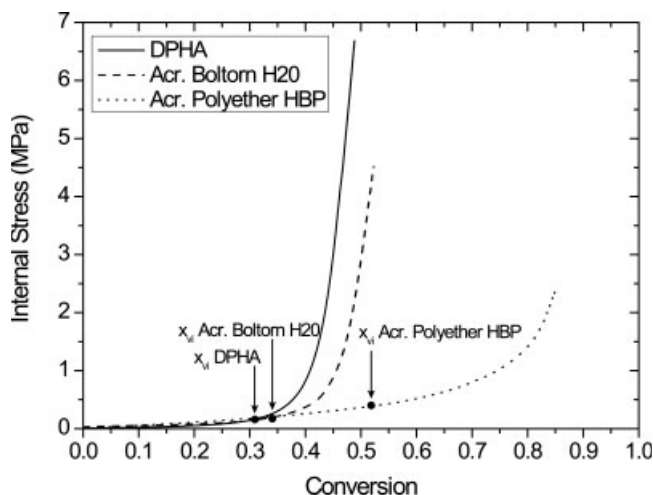


**Figure 4** Internal stress as a function of conversion. Vitrification onset was determined according to the criterion proposed by Wen et al.<sup>37</sup>

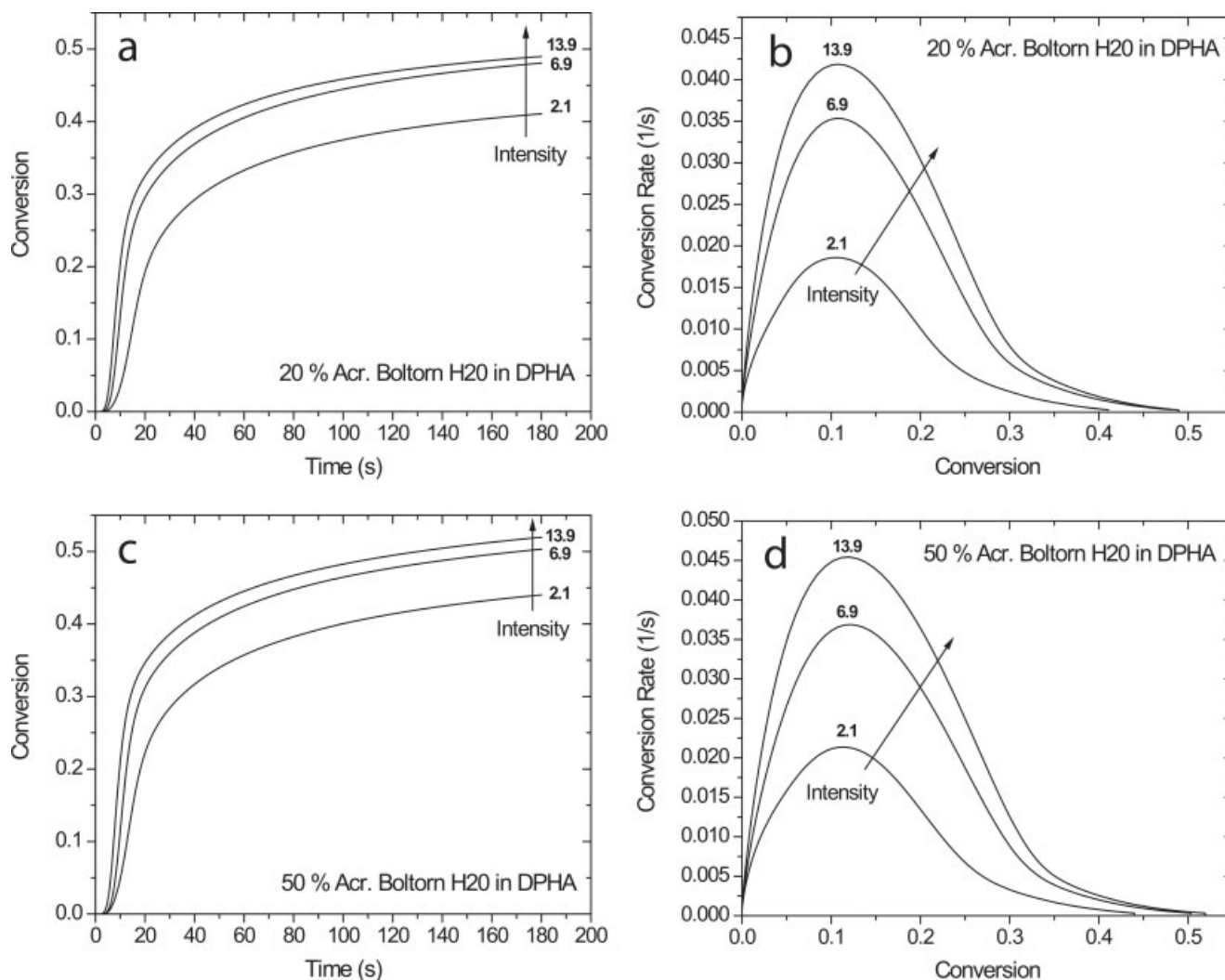


**Figure 5** (a, c) Double bond conversion as a function of time, and (b, d) conversion rate as a function of conversion for different UV intensities ( $\text{mW}/\text{cm}^2$ ), and different Acrylated Boltorn H20 concentrations in DPHA.

using mechanistic or phenomenological models. Mechanistic models, which take into account the processes leading up to polymerization of the system, include the diffusion-controlled nature of the polymerization of highly functional monomers.<sup>31</sup> Phenomenological models are more general and only look at the overall reaction. They are used, for example, when the termination mechanism is not known.

One phenomenological model successfully applied to UV curing of acrylates was the autocatalytic model:<sup>38–40</sup>

$$\frac{dx}{dt} = K \left(1 - \frac{x}{x_m}\right)^n \left(\frac{x}{x_m}\right)^m \quad (1)$$

where  $x$  is the conversion,  $x_m$  represents the maximum conversion obtained in isothermal cure,  $K$  is a rate constant,  $n$  the reaction order, and  $m$  the autocatalytic exponent that stands for the autoacceleration

of the UV reaction,<sup>41</sup> i.e., the immobilization of the reactive chain ends due to an increase in viscosity, resulting in a drop in the termination rate. This model was derived from the autocatalytic Kamal model,<sup>42</sup> which was developed for the thermal cure of polyesters. Although the photopolymerization of acrylates is not autocatalytic but autoaccelerated, these models are well suited for describing this class of reactions provided that the system does not vitrify. After vitrification, the volume relaxation is retarded with respect to chemical conversion, providing excess volume for diffusion, which is not accounted for in this model. Therefore the measured conversion profiles were only modeled from zero conversion to conversion at vitrification onset  $x_{vi}$ . A selection of model conversion curves are compared with measured conversion data in Figure 2.

The influence of intensity  $I$  on the reaction rate  $K$ , the conversion at vitrification  $x_{vi}$ , and the maximum

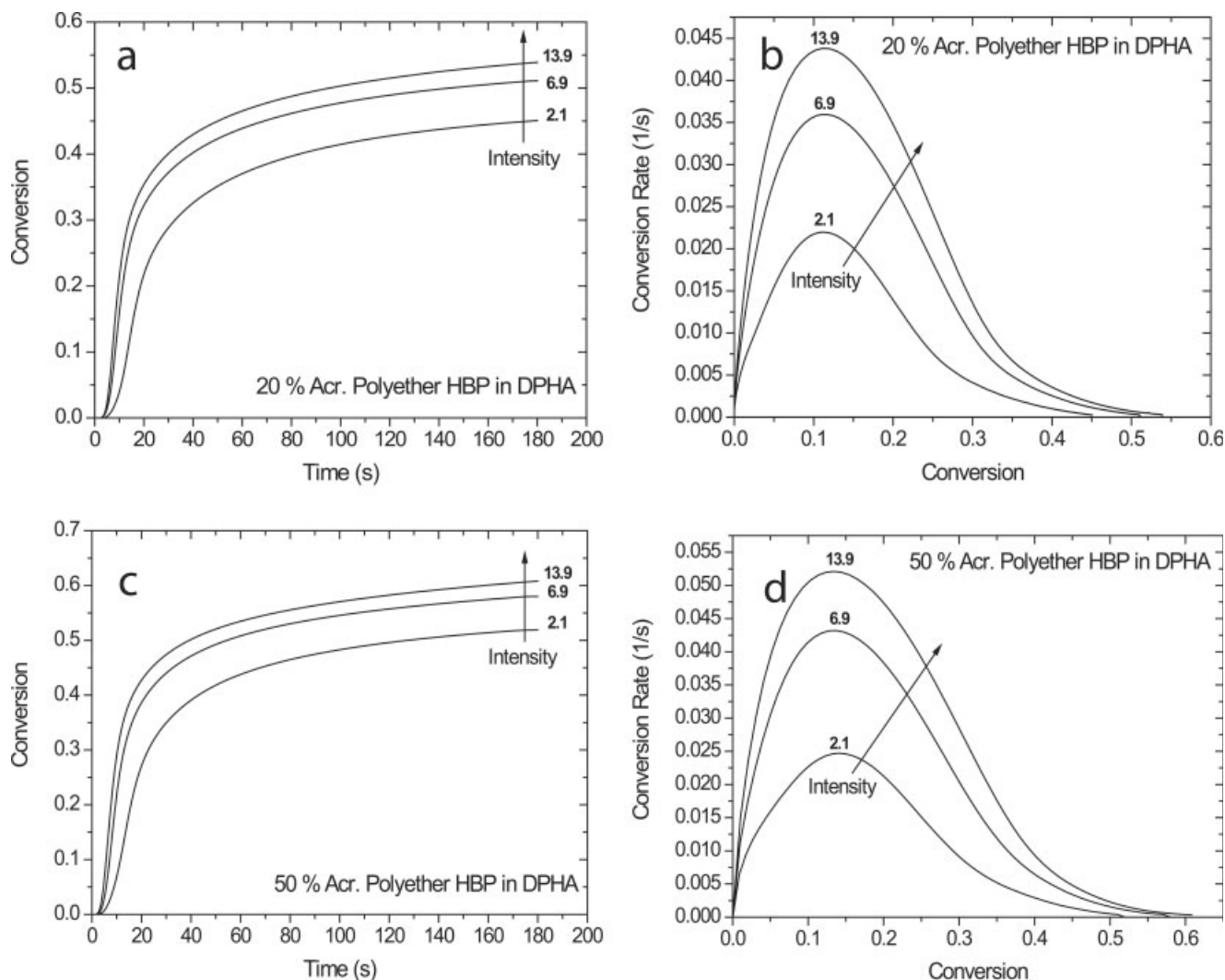


**Figure 6** (a, c) Double bond conversion as a function of time, and (b, d) conversion rate as a function of conversion for different UV intensities (mW/cm<sup>2</sup>), and different Acrylated Polyether HBP concentrations in DPHA.

conversion  $x_m$  was modeled assuming power law behavior:

$$K(I) : I^{\beta_1} \quad (2)$$

$$x_{vi}(I) : I^{\beta_2} \quad (3)$$

$$x_m(I) : I^{\beta_3} \quad (4)$$

where the exponent  $\beta_1$  is related to the termination mechanism,  $\beta_2$  and  $\beta_3$  are empirical constants. For  $\beta_1 < 0.5$ , second order and primary radical termination is predominant (reaction of an initiator radical with a radical site on the evolving polymer). For  $\beta_1 = 0.5$  second order is predominant (reaction of two radical polymer sites). For  $0.5 < \beta_1 < 1$ , first order (e.g., trapping of the radical end in the forming network, or recombination with oxygen) and second order termination happen in parallel. For  $\beta_1 = 1$ , first order termination is predominant.<sup>28,43</sup>

### Influence of composition

The influence of the blend composition on rate constant, conversion at vitrification, and maximum conversion are shown in Figures 7 and 8. Since DPHA and Acrylated Boltorn H20 react in a similar manner, and both vitrify during UV polymerization, the rate constant varies only to a small extent. The reaction order and autocatalytic exponents are found to be close to 2 and 1, respectively, so that the overall reaction order is approximately 3, in agreement with previous analysis of dimethacrylate oligomers.<sup>41</sup>

For the maximal conversion reached, the value of 50% Acrylated Boltorn H20 concentration in DPHA lies above the value for the pure product [Fig. 7(c)]. This result explains why the Young's modulus of the 1/1 Acrylated Boltorn H20/DPHA blend (5.0 GPa) was found to be higher than that of either pure DPHA (3.2 GPa) or pure Acrylated Boltorn H20 (3.9 GPa).<sup>44</sup> The higher conversion of the blend results

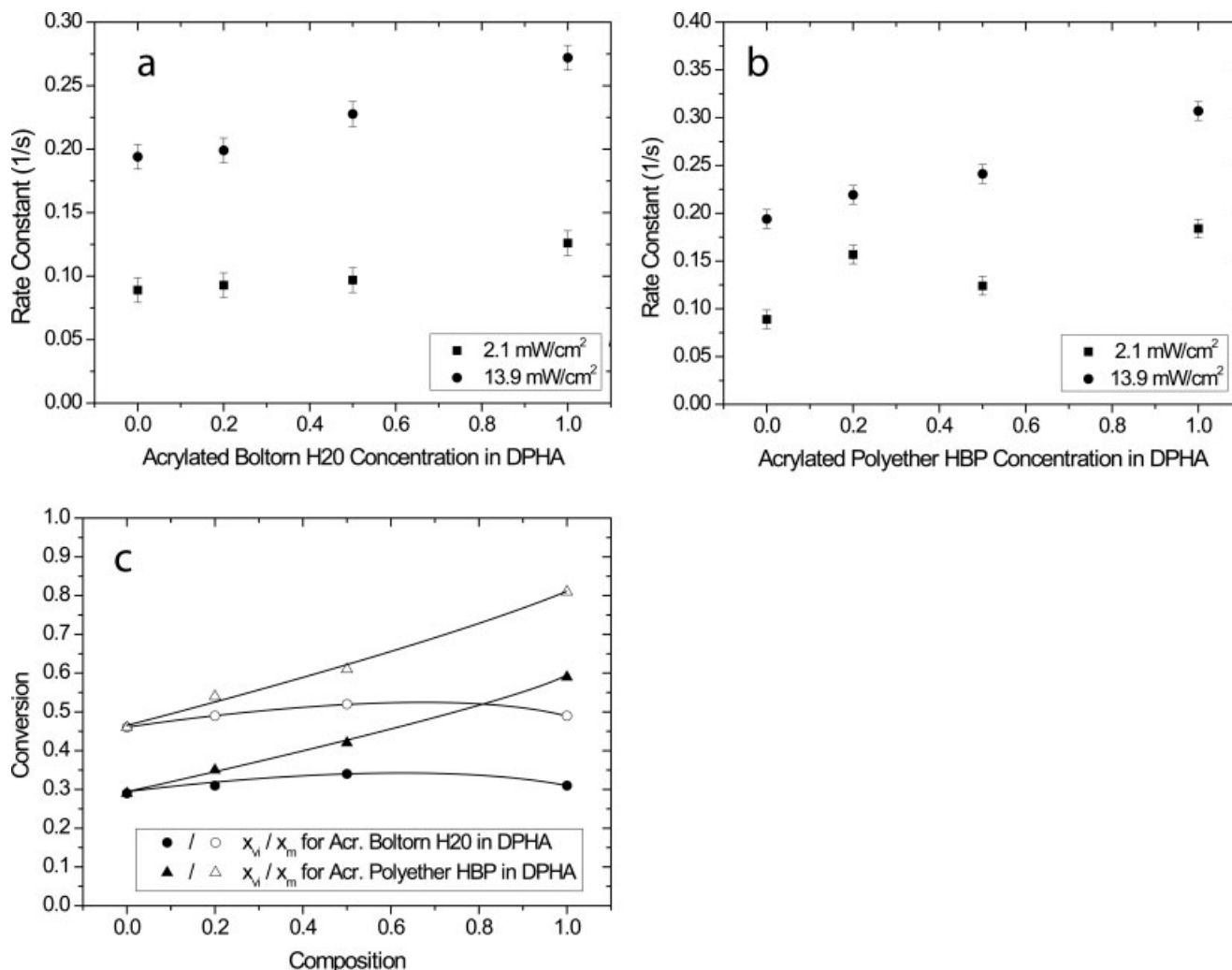


**Figure 7** Dependence of the rate constant  $K$  on (a) the Acrylated Boltorn H20 concentration in DPHA, and (b) the Acrylated Polyether HBP concentration in DPHA at an intensity of 2.1 and 13.9 mW/cm<sup>2</sup>, and dependence of the conversion at vitrification and maximum conversion (c) on the HBP concentration in DPHA (6.8 mW/cm<sup>2</sup>). Lines are guides for the eye.

from the combined synergetic action of increased network mobility and related lower unsaturation concentration compared to DPHA, and reduced viscosity compared to Acrylated Boltorn H20. A similar trend was found for a reactive blend of an acrylated HBP with TMPTA<sup>17</sup> and for HBP-containing epoxy formulations.<sup>12</sup>

For the reactive blend of DPHA with Acrylated Polyether HBP, an increase in the rate constant and in the maximum attainable conversion was observed. This increase results again from a reduction in viscosity of the monomer blend, compared to that of pure DPHA.

Interestingly, for all investigated compositions, the maximum conversion was systematically 16% higher than the conversion at vitrification [Fig. 7(c)]. The  $T_g$  of the acrylate blends at conversion levels between 50% and 83% is reported in Table II. Apart for the blend with 20% of Acrylated Polyether in DPHA, and in spite of different conversion states of the polymers, the  $T_g$  roughly follows the rule of mixtures. This result supports the conversion data shown in Figure 7(c) for the Acrylated Polyether blends (i.e., higher ultimate  $T_g$  implies lower conversion at vitrification during isothermal cure below ultimate  $T_g$ ,

**TABLE II**  
Glass Transition Temperatures and Conversions of Acrylates and Their Reactive Blends

	DPHA	Acr. Boltorn H20	Acr. Polyether HBP	0.2 Acr. Boltorn H20 in DPHA	0.5 Acr. Boltorn H20 in DPHA	0.2 Acr. Polyether HBP in DPHA	0.5 Acr. Polyether HBP in DPHA
$T_g$ (°C)	68	126	28	75	80	105	64
Conversion (%)	73	79	83	50	63	62	64



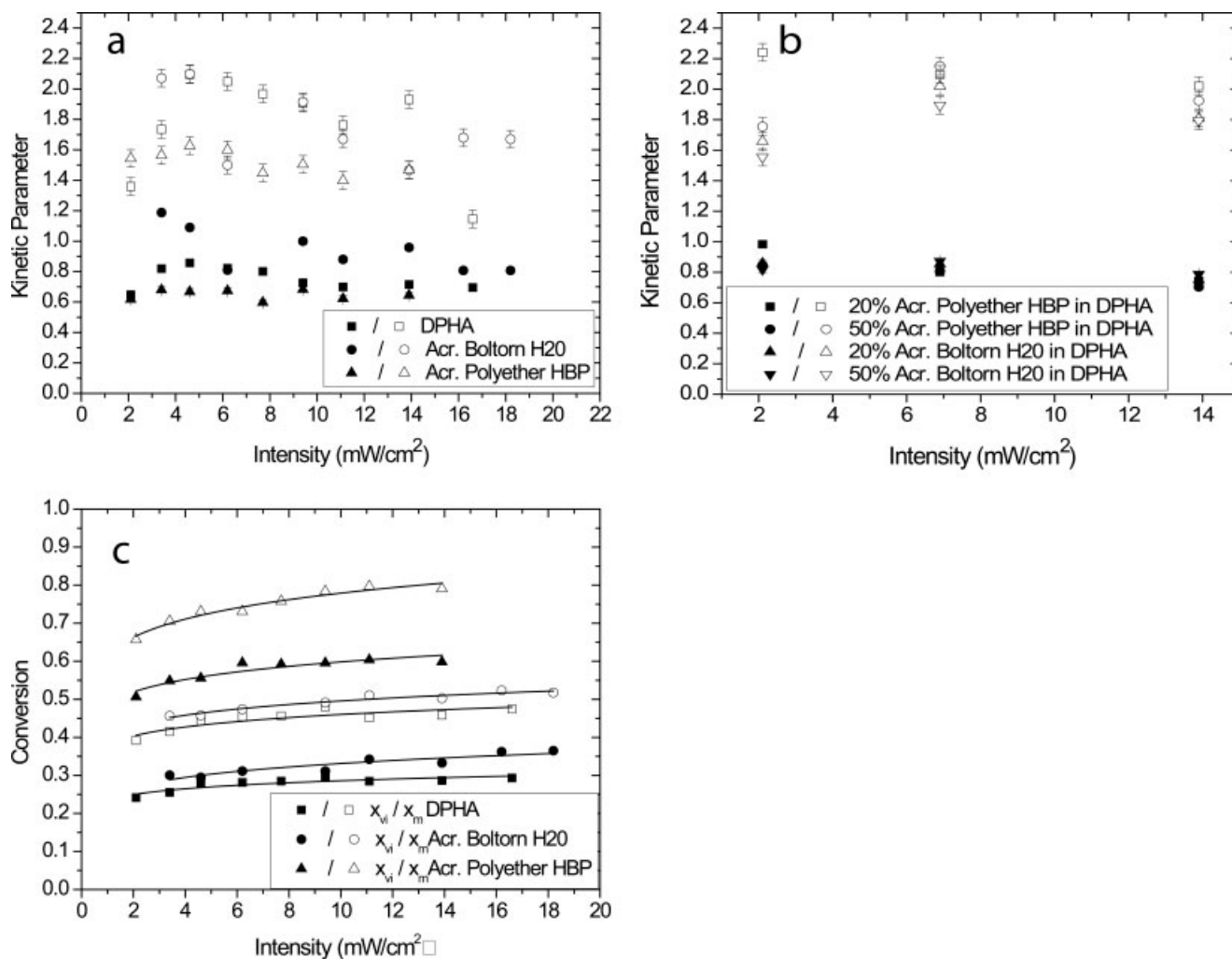


**Figure 8** Influence of intensity on kinetic parameters (reaction order exponent: open symbols; autocatalytic exponent: filled symbols) for pure monomers (a), and their blends (b), and on conversion at vitrification and maximum conversion of the three materials (c). Lines are guides for the eye.

hence lower final conversion), although this trend is not as clear for the acrylated Boltorn H20 blends.

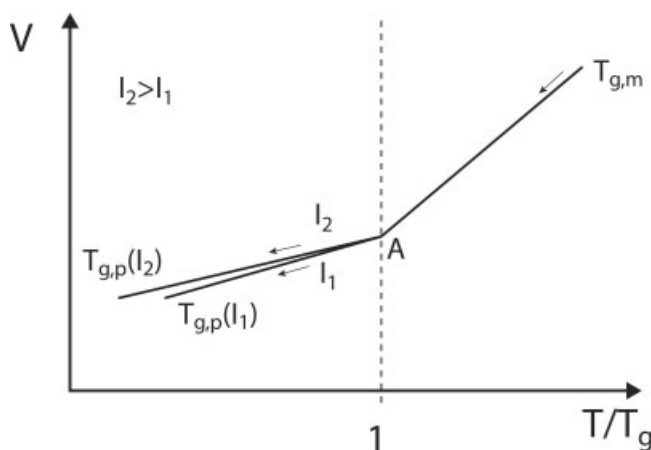
### Influence of intensity

Figure 8 displays the influence of UV intensity on the reaction order, autocatalytic exponents, and on the conversion at vitrification and maximum conversion of all acrylate materials. The reaction order and the autocatalytic exponents are independent of intensity within experimental scatter. As listed in Table III, for all three pure materials, the intensity exponents  $\beta_1$  for the reaction rate were found to be smaller than 0.5. This result is in agreement with a similar study<sup>45</sup> on multifunctional acrylates, thus indicating the predominance of primary radical termination (reaction of radicals attached to the forming macromolecule with small, mobile, initiator-derived radicals), and second order termination. The lower value of 0.29 for Acrylated Polyether HBP,

compared to 0.35 for DPHA and 0.41 for Acrylated Boltorn H20, indicates that first order termination is more prevalent in Acrylated Polyether HBP, whereas the value of 0.41 for Acrylated Boltorn H20 indicates that in this case second order termination is more frequent. In Acrylated Boltorn H20, a high concentration of acrylate functions is not only present on

**TABLE III**  
Rate Constant Exponent  $\beta_1$ , Conversion at Vitrification Exponent  $\beta_2$ , and Maximum Conversion Exponent  $\beta_3$  for Different Materials

	$\beta_1$	$\beta_2$	$\beta_3$
DPHA	0.37	0.084	0.081
Acr. Boltorn H20	0.42	0.127	0.086
20% Acr. Boltorn H20 in DPHA	0.41	0.093	0.061
50% Acr. Boltorn H20 in DPHA	0.41	0.110	0.057
Acr. Polyether HBP	0.25	0.088	0.087
20% Acr. Polyether HBP in DPHA	0.39	0.114	0.053
50% Acr. Polyether HBP in DPHA	0.41	0.101	0.047



**Figure 9** Representation of an isothermal curing cycle in a  $V$  versus  $T/T_g$  diagram for two different intensities ( $V$  is volume,  $T$  is temperature). See text for details.

the surface but also in the core of the molecule, so that second order intramolecular termination is very likely. In contrast, the maximum attainable conversion increases moderately with increasing intensity.

The intensity exponents for conversion at vitrification,  $\beta_2$ , and maximal conversion,  $\beta_3$ , were found to be in the range 0.05–0.13 (Table III), indicating weak intensity dependence, as has already been found elsewhere,<sup>18,29</sup> ( $\sim 0.09$  and  $0.1$ ). And again, final conversion was found to be close to 16% higher than the conversion at vitrification, independent of intensity.

### Photopolymerization of glass-forming systems

The above findings (weak intensity dependence of conversion at vitrification and maximum conversion, and conversion offset between vitrification and final conversion independent of composition and intensity) are related to the interplay between conversion, intensity, and volume of the polymerizing substance, which is unable to keep up the chemical conversion upon vitrification.<sup>16</sup> We propose to illustrate this structural recovery process during UV curing, analogous to physical aging of cured polymers, in the form of an isothermal  $V$  versus  $T/T_g$  diagram (Fig. 9), where  $V$  stands for volume and  $T$  for temperature. This representation resembles the classic volume–temperature diagram for glass forming substances, although it is fundamentally different since  $T$  is constant and  $T_g$  changes with conversion, so that the slopes in Figure 9 are not equal to the coefficients of thermal expansion of the liquid and glassy states. In this representation of isothermal cure, the glass transition temperature is increasing from the glass transition temperature of the monomer  $T_{g,m}$  to the glass transition temperature of the polymer  $T_{g,p}$ , which is a function of conversion, hence of intensity. When the polymer starts to cure, the mobility is high

enough, and the rate of volume shrinkage matches the conversion rate. However, as soon as the curing polymer vitrifies, i.e., when actual  $T_g$  becomes equal to the cure temperature ( $T/T_g = 1$ ), excess volume appears as volume relaxation lags behind conversion.<sup>18,29</sup> This excess volume increases with increasing intensity due to higher conversion rate.<sup>16</sup> After vitrification, the polymer continues reacting until its mobility becomes small enough to stop diffusion. At a given volume, the polymer cured at the higher light intensity  $I_2$  will therefore have a higher ultimate conversion, being responsible for a higher  $T_g$ , compared to that cured under intensity  $I_1$ .

Increasing intensity is indeed generally used to reach higher conversions, although it is essentially useful to speed up the reaction. To reach a high ultimate conversion, further factors as photoinitiator concentration and temperature (i.e., increased mobility) are therefore more effective, at least to a certain optimum, beyond which the maximum conversion decreases again.<sup>46</sup>

### CONCLUSIONS

The influence of intensity and vitrification on the UV curing behavior of DPHA; two acrylated HBPs, one with a stiff polyester and one with a flexible polyether structure; and DPHA/HBP reactive blends was investigated.

An autocatalytic model was used up to the onset of vitrification, which was determined from the conversion rate behavior, with a power-law intensity dependence of the reaction rate, conversion at vitrification, and ultimate conversion. It was found that the reaction order and autocatalytic exponents were independent of intensity and close to 2 and 1, respectively, for all materials. The power law exponent describing the influence of intensity on the reaction rate was about 0.4 for all compositions, thereby suggesting that the main termination mechanisms were a combination of second order and primary radical termination.

Ultimate conversion was found to be 0.16 higher than conversion at vitrification for all investigated materials and blends independent of UV intensity, which was argued to result from volume relaxation processes in the vitrifying acrylates.

The authors thank Dr. André Fuchs from Ciba Specialty Chemicals for useful advice and the Laboratoire de Polymères (EPFL) for access to their DSC and FTIR.

### References

1. Davidson, S. *Exploring the Science, Technology and Applications of UV and EB Curing*; SITA Technology: London, UK, 1999.

2. Francis, L. F.; McCormick, A. V.; Vaessen, D. M.; Payne, J. A. *J Mater Sci* 2002, 37, 4717.
3. Patel, M. P.; Braden, M.; Davy, K. W. M. *Biomaterials* 1987, 8, 53.
4. Sato, K. *Prog Org Coat* 1980, 8, 143.
5. Negele, O.; Funke, W. *Prog Org Coat* 1996, 28, 285.
6. Luciani, A.; Plummer, C. J. G.; Gensler, R.; Månson, J.-A. E. *J Coat Technol* 2000, 72, 161.
7. Klee, J. E.; Schneider, C.; Hölter, D.; Burgath, A.; Frey, H.; Mülhaupt, R. *Polym Adv Technol* 2001, 12, 346.
8. Kou, H.-G.; Asif, A.; Shi, W.-F. *Chin J Chem* 2003, 21, 91.
9. Wan, Q.; Schrickler, S. R.; Culbertson, B. M. *J Macromol Sci Pure A* 2000, 37, 1317.
10. Eom, Y.; Boogh, L.; Michaud, V.; Månson, J.-A. E. *Polym Compos* 2002, 23, 1044.
11. Mezzenga, R.; Plummer, C. J. G.; Boogh, L.; Månson, J.-A. E. *Polymer* 2000, 42, 305.
12. Sangermano, M.; Malucelli, G.; Bongiovanni, R.; Priola, A.; Harden, A.; Rehnberg, N. *Polym Eng Sci* 2003, 43, 1460.
13. Xu, G.; Shi, W. *Prog Org Coat* 2005, 52, 110.
14. Johansson, M.; Glauser, T.; Rospo, G.; Hult, A. *J Appl Polym Sci* 2000, 75, 612.
15. Claesson, H.; Malmström, E.; Johansson, M.; Hult, A.; Doyle, M.; Månson, J. A. E. *Prog Org Coat* 2002, 44, 63.
16. Cook, W. D. *Polymer* 1992, 33, 600.
17. Kou, H.; Asif, A.; Shi, W. *J Appl Polym Sci* 2003, 89, 1500.
18. Bowman, C. N.; Peppas, N. A. *Macromolecules* 1991, 24, 1914.
19. Lange, J.; Månson, J.-A. E. *Polymer* 1996, 37, 5859.
20. Lange, J.; Altmann, N.; Kelly, C. T.; Halley, P. J. *Polymer*, 2000, 41, 5949.
21. Schmidt, L. E.; Leterrier, Y.; Vesin, J.-M.; Wilhelm, M.; Månson, J.-A. E. *Macromol Mater Eng* 2005, 290, 1115.
22. Malmström, E.; Johansson, M.; Hult, A. *Macromolecules* 1995, 28, 1698.
23. Magnusson, H.; Malmström, E.; Hult, A. *Macromol Rapid Commun* 1999, 20, 453.
24. Hoyle, C. E. In *Radiation Curing: Science and Technology*; Pappas, S. P., Ed.; Plenum: New York, 1992; p 57.
25. Hill, L. W. In *Paint and Coating Testing Manual*; Koleske, J. V., Ed.; ASTM: Philadelphia, 1995; p 534.
26. Anseth, K. S.; Bowman, C. N.; Peppas, N. A. *Polym Bull* 1993, 31, 229.
27. Stoney, G. G. *Proc R Soc London Ser A* 1909, 82, 172.
28. Andrzejewska, E. *Prog Polym Sci* 2001, 26, 605.
29. Kloosterboer, J. G. *Adv Polym Sci* 1988, 84, 1.
30. Cook, W. D. *Polymer* 1992, 33, 2152.
31. Kurdikar, D. L.; Peppas, N. A. *Macromolecules* 1994, 27, 4084.
32. Hayden, P.; Melville, S. H. *J Polym Sci* 1960, 43, 215.
33. Dietz, E. J.; Peppas, N. A. *Polymer* 1997, 38, 3767.
34. Yu, Q.; Nauman, S.; Santerre, J. P.; Zhu, S. *J Mater Sci* 2001, 36, 3599.
35. Payne, J. A. PhD Thesis, Department of Chemical Engineering and Materials Science; University of Minnesota: Twin Cities, 1998.
36. Payne, J. A.; Francis, L. F.; McCormick, A. V. *J Appl Polym Sci* 1997, 66, 1267.
37. Wen, M.; Scriven, L. E.; McCormick, A. V. *Macromolecules* 2002, 35, 112.
38. Chandra, R.; Soni, R. K. *Polym Int* 1993, 31, 239.
39. Chandra, R.; Soni, R. K.; Murthy, S. S. *Polym Int* 1993, 31, 305.
40. Andrzejewska, E.; Bogacki, M. B.; Andrzejewski, M. *Polimery (Warsaw)* 2001, 46, 549.
41. Andrzejewska, E.; Lindén, L.-Å.; Rabek, J. F. *Polym Int* 1997, 42, 179.
42. Kamal, M. R.; Sourour, S. *Polym Eng Sci* 1973, 13, 59.
43. Timpe, H.-J.; Strehmel, B. *Macromol Chem Phys* 1991, 192, 779.
44. Schmidt, L. E.; Leterrier, Y.; Schmaeh, D.; Månson, J.-A. E.; James, D. In *RadTech Europe Conference, Barcelona, 2005*; p 385.
45. Timpe, H.-J.; Strehmel, B.; Roch, F. H.; Fritzsche, K. *Acta Polym* 1987, 38, 238.
46. Lecamp, L.; Youssef, B.; Bunel, C. *Polymer* 1997, 38, 6089.